Fabrication of Nanoscale Columnar Diodes by Glancing Angle Deposition

Jacob Weightman[1]
[1] *Dept. of Physics and Astronomy, Macalester College: St. Paul, MN*

ABSTRACT

Glancing angle deposition (GLAD) is a process in which thin films are deposited onto a substrate with obliquely incident vapor together with precisely controlled azimuthal substrate rotation. Ballistic shadowing effects due to the oblique incidence produce nanoscale structures, and a variety of feature shapes, including tilted columns, helices, and vertical columns can be achieved by varying the azimuthal rotation during the deposition process. Due to this control of morphology and the compatibility of the process with a wide variety of materials, GLAD films have found applications in a variety of fields including sensing, photonics, photovoltaics, and catalysis, where they are predominantly used as coatings with tunable optical, mechanical, and chemical properties. However, there has been little work regarding its use for the fabrication of electronic devices. GLAD films are interesting in this respect because it would enable nanoscale devices to be made without lithography. We propose a method for fabricating vertically-aligned, columnar Schottky diodes by GLAD. We then fabricate these devices using electron beam evaporation of chromium onto a silicon substrate, with chromium and aluminum contacts, and characterize these devices by SEM and I-V curve measurements.

I. INTRODUCTION

For many applications, it is desirable to create thin films of regular nanoscale structures with tunable morphology. One fabrication technique for fabricating such films is called Glancing angle deposition (GLAD), whereby obliquely incident vapor condenses onto a substrate with precisely controlled azimuthal orientation. GLAD films have been used for many applications, including humidity[1] and pressure sensors[2], waveguides[3], and antireflection coatings on solar cells[4]. For the first time, we attempt to create electronic semiconductor devices using

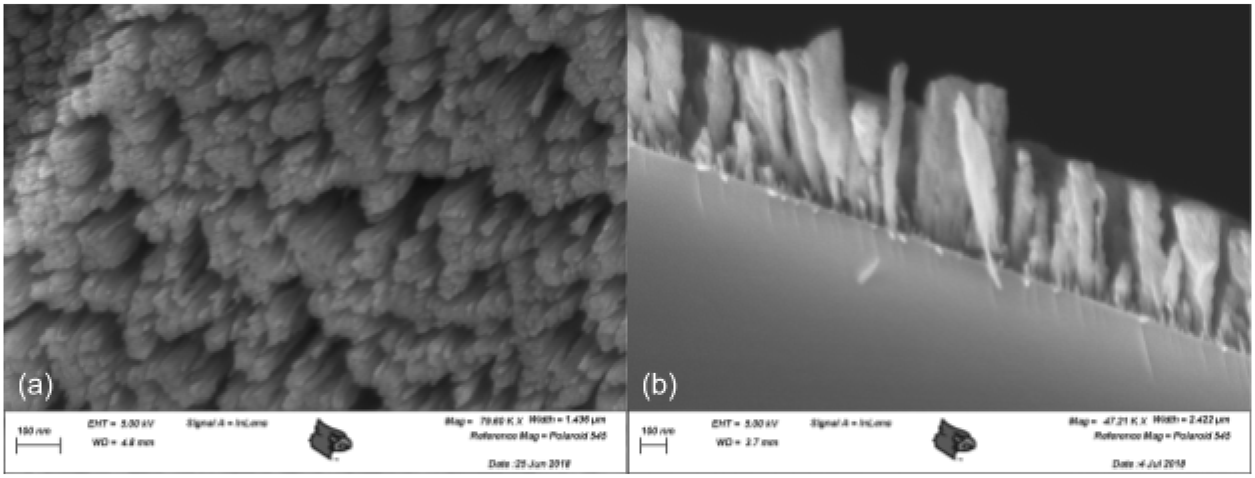

Fig 1. SEM images of a GLAD film made with Cr metal on a polished Si 001 wafer. The vapor was incident at 84° from normal, and there was no substrate rotation. (a) The film viewed from normal incidence and (b) a cross-section of the same film. Note that this produced a film of tilted column structures roughly 50-150 nm wide.

GLAD. We believe that GLAD might be an interesting fabrication technique in this area because it would allow the simultaneous fabrication of nanoscale structures with high areal density in a single fabrication step. This might be advantageous over traditional lithography due to its simplicity and lower equipment costs.

One requirement for GLAD is that the incident vapor has a mean free path length comparable to the separation of the target and substrate, which may be achieved by a number of deposition techniques under high vacuum, including electron beam evaporation (ebeam) deposition [5], thermal evaporation deposition [6], and magnetron sputtering [2]. Due to the facilities available for the present study, we concern ourselves exclusively with ebeam deposition.

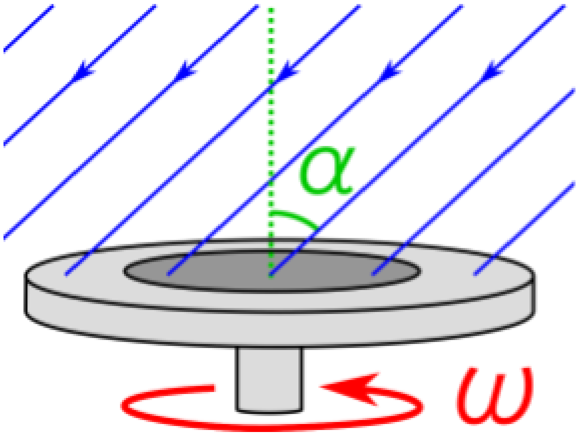

Fig 2. An illustration of a GLAD setup, with the vapor incidence angle, α, and azimuthal angular velocity, ω, shown.

If the mean free path of particles of the target material in the deposition chamber is comparable to or larger than the target-substrate separation, then a significant fraction of the incident particles will not scatter before condensing onto the substrate, and will follow a "line of sight" path instead. These particles tend to deposit onto the substrate near where they first strike it, and so any features on the surface of the substrate will occlude areas behind them, so these areas of the substrate will not receive new material. Due to the very oblique angle of incidence—typically more than 75° from the substrate normal—the areas occluded by surface features are much larger than the features themselves. This effect is called ballistic shadowing [7]. If the substrate is rotated during the deposition, the areas that are shadowed will change. As a result, manipulating the azimuthal rotation of the substrate controls the shape of the resulting nanostructures. It is worth noting that ballistic shadowing also requires that the temperature of the substrate is small compared to the melting point of the target material; if it is not, then deposited atoms will quickly diffuse on the surface away from their initial point of impact, allowing material to accumulate in shadowed regions. This is not an issue for GLAD films of many materials; for example, the homologous temperature of chromium at room temperature is 0.14 [8].

There are several variables of interest in controlling the properties of the films during fabrication. These include: the incidence angle of the vapor, α, measured between the vapor flux vector and substrate normal; the azimuthal angle, θ; and the vapor flux density (Fig. 2). In general, all of these quantities may be changed over time during the deposition. For our purposes, it is more useful to use the azimuthal angular velocity, ω. It has been found that larger values of α, corresponding to more oblique incidence angles, produces more oblique columns [5]. The relationship between α and column tilt angle is non-linear, and a variety of geometric and physical models[9] for this behavior have been proposed with varying levels of agreement in different ranges of incidence angles [10]. It is also known that larger values of α at the same flux density also produce thinner films due to reduced vapor flux per substrate area, greater separation between columns, and narrower columns, all else being equal [5].

Manipulating the azimuthal rotation over the course of the deposition will sculpt the nanostructures into one of many different shapes. With a constant azimuthal angle, a film of tilted columns is deposited, oriented toward the incident vapor (Fig. 1). If the azimuthal angle is abruptly changed, new columns will grow on top of the old ones, oriented in the new direction of incident vapor, producing a chevron shape. Continuously varying the azimuthal angle produces a continuum of growth directions, and thus grows curved structures (Fig 7). Rotation with a constant angular velocity will produce helical nanostructures, with slow rotations producing wide helices and fast rotations producing narrow helices. Very fast rotations will produce vertical columns, since the radius of the helix is small compared to the width of the structure [8].

In the present study, we fabricate vertical columnar diodes using GLAD. Schottky diodes are a semiconductor device which consists of a single junction between a metal and a semiconductor. In an ideal Schottky diode, the mismatch in work functions of the metal and semiconductor cause the bands of available states to bend such that the majority carriers in the semiconductor face a potential barrier at the interface. Changing the electrical bias of the interface changes the size of this barrier, such that in "forward bias" the majority carrier readily flows from the semiconductor to the metal, and in "reverse bias" the flow is inhibited by the barrier. In the ideal case, the current varies exponentially with the junction voltage. An overview of the semiconductor physics of Schottky diodes can be found in [11].

II. METHODS

For simplicity, we fabricate Schottky diodes with chromium, but the technique presented here could be adapted to produce P-N diodes by depositing a semiconductor instead of a metal. By depositing a metal GLAD film onto a semiconducting substrate, a Schottky junction is formed where the deposited structures meet the substrate. We chose to use chromium metal and p-type silicon for these diodes because of chromium's ease of use with our ebeam deposition system, and because of the ease of making ohmic contact to p-type silicon compared to n-type with the facilities available.

First, in order to select good deposition parameters for later steps, we deposited several films with deposition angles ranging from 78º to 84º and azimuthal rotation rates ranging from 0 to 0.2 RPM, while holding constant the deposition duration at 40 minutes and deposition rate at roughly 5 nm/s for normal incidence, as measured by a quartz crystal sensor in the deposition chamber. Similarly to [5], we found that more oblique deposition angles resulted in wider column spacing and thinner films. We observed tilted columns for the depositions with $\omega = 0$ RPM, relatively large radius helices with $\omega = 0.1$ RPM, and relatively small radius helices with $\omega = 0.2$ RPM. We also found that faster azimuthal rotation rates produced thinner films. Simple 2-probe electrical continuity measurements revealed that the α=78º film was continuous, so that a current may easily flow between two points on its surface, while the α=84º film was discontinuous. In order to produce many distinct diodes on the surface and maximize the thickness of the film, we chose to use a very oblique angle and moderate rotation speed.

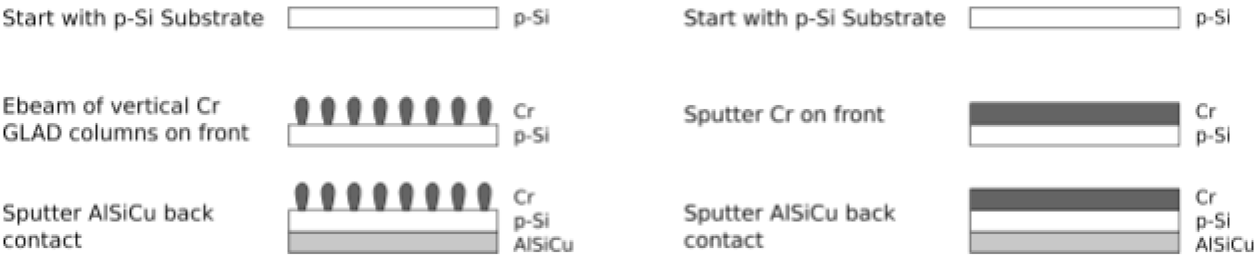

Fig 3. The fabrication procedures for the GLAD diodes (left) and planar diodes (right). The Cr/p-type Si junction is a schottky junction, while the p-type Si/AlSiCu alloy junction is ohmic. The GLAD film comprises many tightly-wound helical structures.

We then prepared two kinds of diodes (Fig 3): our GLAD Schottky diodes, and a sputtered planar diode using the same materials as a reference device. We prepared p-type Si (100) wafers by immersing them in a buffered HF solution for 2 minutes, followed by three immersion cycles in deionized water and spun dry in order to remove any oxide layer that had formed on the surface. For the GLAD diodes, we then loaded the wafer into the ebeam system and deposited a film of Cr metal using α=84º and ω = 0.1 RPM for 50 minutes with a deposition rate corresponding to of 5±1 nm/s growth normally incident on the film thickness sensor. This film was deposited on the polished side of the wafer. We then immediately sputtered the reverse side of the wafer with an alloy of Al (98.5%), Si (1%), Cu (0.5%) using Ar gas at a pressure of 5.0×10^{-3} torr and 500 W for 25 minutes in order to form an ohmic back contact. Based on previous characterization of this process in our lab, we estimate that this film is 300 nm thick. For the reference diode, we followed an identical process for cleaning and sputtering the back contact, but instead sputtered a chromium film onto the polished side of the wafer. This was done using Ar gas at a pressure of 5.0×10^{-3} torr and 300 W for 25 minutes.

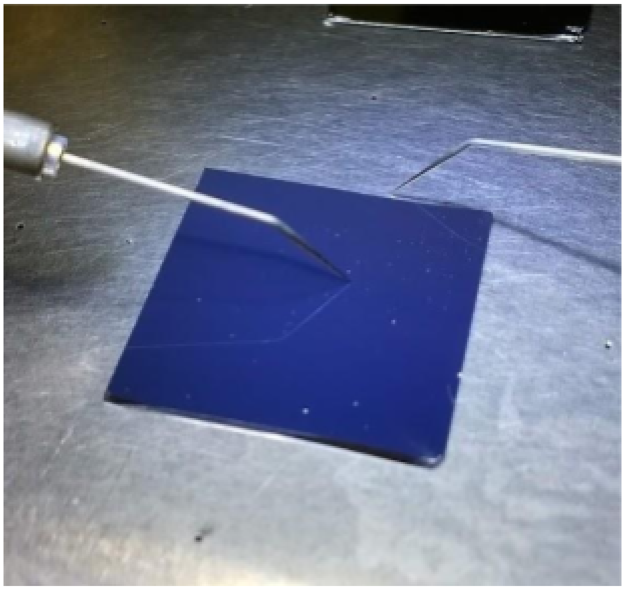

Fig 4. The probe configuration for I-V curve measurements on a Cr GLAD diode.

The GLAD diode and sputtered planar diode wafers were cleaved into square 4 cm^2 pieces in preparation for current-voltage (I-V) curve measurements. These measurements were made with 100 μm tungsten probe tips at a probe station. The devices were placed on a large stainless steel vacuum chuck and held in place with suction, with one probe placed directly onto the chuck close to the sample to make electrical contact to the AlSiCu back contact, and the other probe was gently placed directly onto the top film approximately in the center (Fig 4).

Initial measurements showed very strange I-V curves with many inflection points. The devices were then treated with an AC voltage of 75 V RMS at 60 Hz until the I-V curve stabilized. A new I-V curve was measured and saved. This process was carried out without moving the probe tips, so that the final I-V curve was measured on the same GLAD structures that were electrically stressed.

III. RESULTS

Inspection of the Cr GLAD film under SEM revealed apparently isolated metal columns approximately 600 nm tall, 100 nm wide at their widest, and helical in shape with 5 turns. By counting the columns in an SEM image, we estimate the areal density of diodes to be on the order of 10^{11} diodes per square meter (Fig 6).

We found by 2-probe continuity measurements that the sputtered Cr film was electrically continuous, while Cr GLAD diode films were not. Thus, we conclude that the GLAD structures do not electrically short with each other on length scales larger than 1 mm. We expect that they also do not short on shorter length scales, since there is negligible conducting material between them. Based on our cross-section SEM images, there is only a thin layer of metal film a few nanometers thick which likely nucleated early in the deposition which may electrically short between columns.

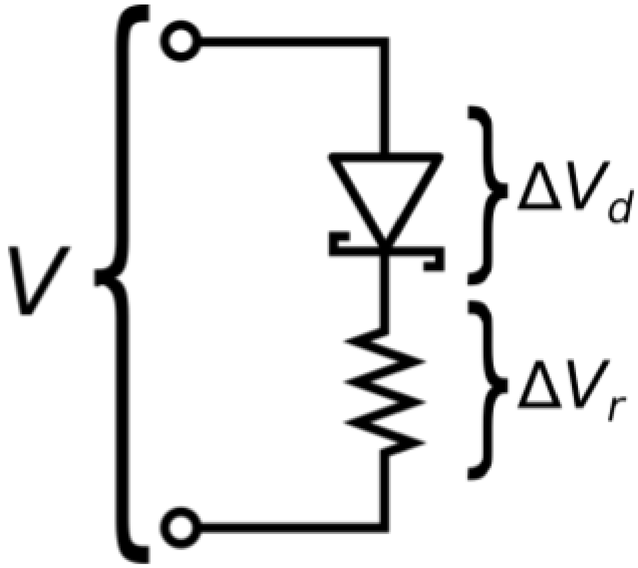

Fig 5. The model used to Describe the fabricated diodes. This model has three free parameters: the ideality factor and reverse saturation current of the diode, and the resistance of the series resistor.

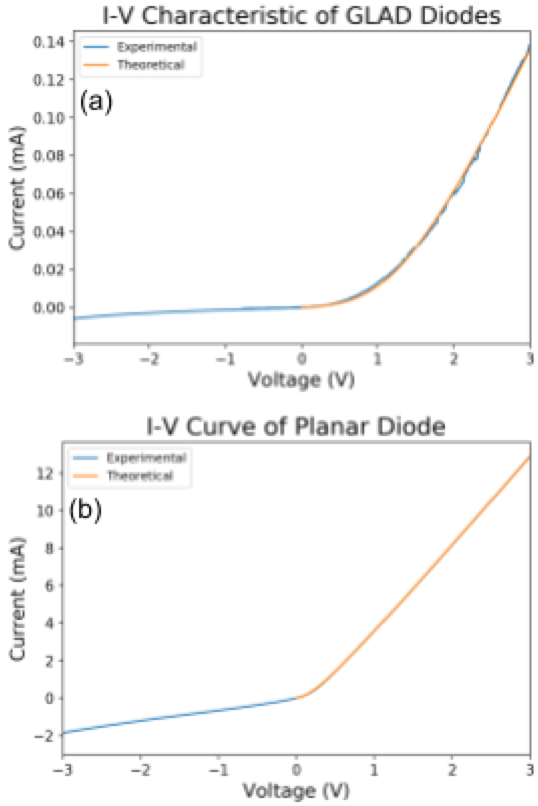

Fig 6. I-V curves of (a) the GLAD diodes and (b) the sputtered diode. Note the roughly exponential behavior near V=0, and linear asymptotes at larger positive and negative voltages. This is the expected behavior of an ideal Schottky diode with a series resistance.

We modeled the I-V curves of our devices as an ideal diode in series with an effective resistance, R_s (Fig 5). We use the Shockley diode equation for the ideal diode, introducing a reverse saturation current, I_s, and ideality factor, η. The ideality factor is typically used to account for geometric non-ideality in diodes; however, here we use it as an empirical fitting parameter to capture non-ideal behavior of our devices. Taking this together with Ohm's law for the series resistance and Kirchhoff's law, we have three equations which must be satisfied:

$$\Delta V_R + \Delta V_d = V$$

$$\Delta V_R = IR_s$$

$$I = I_s(e^{\Delta V_d/\eta V_T} - 1)$$

where V is the voltage across the device, I is the current through the device, ΔV_R is the voltage across the resistor, ΔV_d is the voltage across the diode, and V_T is the thermal voltage which is 25.9 mV at room temperature. Rearranging, we find that

$$V = IR_s + \eta V_T ln(1 + \frac{I}{I_s})$$

Which cannot be solved algebraically for the current. Instead, we solve this equation numerically using the bisection method. We then fit this model to our measured I-V curves using a nonlinear least squares algorithm provided by SciPy [13]. The fitting parameters are shown in Table 1. In an ideal diode, η would be 1, Rs would be 0, and the reverse saturation current would be tunable for the specific application. The reverse saturation currents are not directly comparable between the GLAD diodes and the sputtered diode due to the different shapes of the diodes. In fact, converting the current in the GLAD diodes into a current density which could be compared is nontrivial due to the geometry of the columns—this would require knowing the contact area between the GLAD columns and the substrate, which is complicated by the abundance of small, shadowed columns revealed in SEM that are close to the substrate.

	I_s (A)	**η (dimensionless)**	**R_s (Ω)**
Cr GLAD Diode	$1.75 \pm 0.07 \times 10^{-6}$	16.3 ± 0.2	8260 ± 80
Sputtered Cr Diode	$6.07 \pm 0.04 \times 10^{-5}$	2.527 ± 0.005	205.52 ± 0.05

Table 1. The nonlinear least-squares fit parameters for the GLAD and sputtered Cr/p-Si Schottky diodes. Note the high ideality factor and series resistance of the GLAD diodes.

IV. CONCLUSIONS

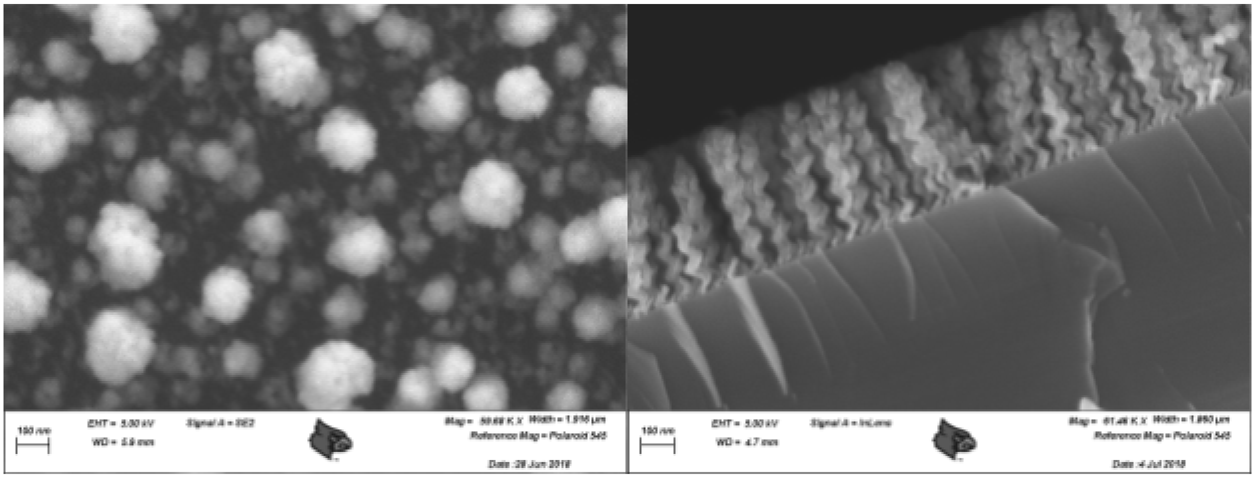

Fig 7. SEM images of GLAD film deposited with $\alpha=84°$ and $\omega=0.1$ *rpm* with 50 minute deposition time. (a) a top view of the film and (b) a cross section of the film.

We have successfully fabricated Schottky diodes using GLAD. These devices are interesting because of the simplicity of their fabrication and high areal density. As far as we know, these are the first semiconductor devices to be made with this process. Characterization by I-V curve measurements indicate that they are relatively non-ideal, with ideality factors roughly 6 times larger than our reference device, perhaps due to porosity of the deposited material, low-quality material interfaces at the metal-semiconductor junction, or the non-ideal geometry of the devices. They also suffer from unacceptably high series resistance, which was roughly 40 times larger than in our reference device. Engineering these devices to reduce series resistance and produce more ideal junctions are opportunities for further work, and are essential to producing high-quality diodes with this technique.

REFERENCES

1. Matthew M. Hawkeye and Michael J. Brett. Optimized Colorimetric Photonic-Crystal Humidity Sensor Fabricated Using Glancing Angle Deposition. *Advanced Functional Materials,* 21(19): 3652-3658, 2011.
2. S. V. Kesapragada, P. Victor, O. Nalamasu, and D. Gall. Nanospring pressure sensors grown by glancing angle deposition. *Nano Letters,* 6(4): 854-857, 2006.
3. M. A. Summers, K. Tabunshchyk, A. Kovalenko, and M. J. Brett. *Fabrication of 2D–3D photonic crystal heterostructures by glancing angle deposition,* 7(2): 76-84, 2009.
4. Yong Jun Park, K. M. A. Sobahan, Jin Joo Kim, and Chang Kwon Hwangbo. Antireflection Coatings with Helical SiO2Films Preparedby Using Glancing Angle Deposition. *Journal of the Korean Physical Society,* 55(6): 2634-2637, 2009.
5. Christina Buzea, Gisia Beydaghyan, Chelsea Elliot, and Kevin Robbie. Control of power law scaling in the growth of silicon nanocolumn pseudo-regular arrays deposited by glancing angle deposition. *Nanotechnology,* 16(10): 1986, 2005.
6. Mary W. Seto, Brian Dick, and Michael J. Brett. Microsprings and microcantilevers: studies of mechanical response. *Journal of Micromechanics and Microengineering*, 11(5):582, 2001.
7. T. Smy, D. Vick, M. J. Brett, S. K. Dew, A. T. Wu, J. C. Sit, and K. D. Harris. Three-dimensional simulation of film microstructure produced by glancing angle deposition. *Journal of Vacuum Science & Technology A: Vacuum, Surfaces, and Films,* 18(5):2507, 2000.
8. S. Liedtke, Ch. Grüner, A. Lotnyk, and B. Rauschenbach. Glancing angle deposition of sculptured thin metal films at room temperature. *Nanotechnology*, 28(38):385604, 2017.
9. Wai-Fung Lau, Fan Bai, and Zhifeng Huang. Ballistic glancing angle deposition of inclined Ag nanorods limited by adatom diffusion. *Nanotechnology*, 24(48): 465707, (2013).
10. Christina Buzea and Kevin Robbie. Nano-Sculptured Thin Film Thickness Variation with Incidence Angle. *Journal of Optoelectronics and Advanced Materials,* 6:1263-1268, 2004.
11. Robert F. Pierret. Semiconductor Device Fundamentals. *Addison-Wesley Publishing,* 1996.
12. K. Robbie. Advanced techniques for glancing angle deposition. *Journal of Vacuum Science & Technology B: Microelectronics and Nanometer Structures,* 16(3):1115 1998.
13. Eric Jones et al. SciPy: Open Source Scientific Tools for Python. 2001.